

Neurofibrillary Tangle-Associated Collapsin Response Mediator Protein-2 (CRMP-2) Is Highly Phosphorylated on Thr-509, Ser-518, and Ser-522

Yongjun Gu,^{‡,§} Naoki Hamajima,^{||} and Yasuo Ihara^{*,‡,§}

Department of Neuropathology, Faculty of Medicine, University of Tokyo, Hongo 7-3-1, Bunkyo-ku, Tokyo 113-0033, Japan, Department of Pediatrics, Nagoya City University Medical School, Mizuho-ku, Nagoya 467-8601, Japan, and Core Research and Evolutional Science and Technology (CREST), Japan Science and Technology Corporation (JST), Kawaguchi, Saitama 332-0012, Japan

Received October 6, 1999; Revised Manuscript Received January 4, 2000

ABSTRACT: 3F4, a monoclonal antibody raised against partially purified paired helical filaments (PHFs), strongly labeled neurofibrillary tangles and some plaque neurites but barely labeled neuropil threads. The levels of the 65-kDa antigen were significantly increased in the soluble fraction of the brains affected by Alzheimer's disease (AD), as compared with that in the case of control brains. The antigen was previously identified as human collapsin response mediator protein-2 (hCRMP-2) by sequencing the immunoaffinity-purified 65-kDa antigen [Yoshida, H., Watanabe, A., and Ihara, Y. (1998) *J. Biol. Chem.* 273, 9761–9768]. Here, we show that the 3F4 antigen represents a highly phosphorylated form of CRMP-2. The 3F4-reactive phosphoepitope was localized to the carboxyl-terminal portion of hCRMP-2, and was created by a novel 45–50-kDa protein kinase in rat brain extract. Site-directed mutagenesis of this portion showed that multiple sites of CRMP-2 are differentially phosphorylated within residues 507–522, and that phosphorylation of three sites, Thr-509, Ser-518, and Ser-522, is required for full 3F4 binding. The phosphorylation of this particular portion carboxyl-terminal to the basic region of CRMP-2 may play an important role in regulating its activity, and may be involved in the formation of degenerating neurites in AD brain.

The formation of innumerable neurofibrillary tangles (NFTs)¹ throughout the cerebral cortex is one of the neuropathological hallmarks of Alzheimer's disease (AD). The unit fibrils of NFTs are designated as paired helical filaments (PHFs), and their framework is composed of hyperphosphorylated full-length tau (PHF-tau) (1), or processed and smeared tau (2, 3). Although primary significance has been placed on senile plaques in the investigation of the pathogenesis of AD, the density of senile plaques was found not to be related to the extent of neuronal loss in AD brains (4). In contrast, the density of NFTs in AD brains has been repeatedly reported to be well correlated with the extent of neuronal loss and dementia (4). Thus, the intraneuronal formation of PHFs has been considered to be closely related

to neuronal death in AD. This speculation has recently been substantiated by the discovery of a new entity of familial dementia called frontotemporal dementia and parkinsonism linked to chromosome 17 (FTDP-17; 5–7). In this disease, the extensive loss of neurons and the formation of PHF-like fibrils in distinct areas are caused by intronic or exonic mutation of the tau gene (for review, see ref 8).

3F4, a monoclonal antibody, was raised against partially purified PHFs. It intensely stained NFTs and some plaque neurites, but barely stained neuropil threads. Western blotting with 3F4 uncovered a 65-kDa cytosolic protein distinct from tau, and quantitative analysis showed that its levels were significantly increased in the soluble fraction of AD brains as compared with that in the case of control brains (9). Partial sequencing of the purified 3F4 antigen revealed that it was human collapsin response mediator protein-2 (hCRMP-2) (9).

Collapsin response mediator proteins (CRMPs) are a family of cytosolic proteins whose expression patterns are developmentally regulated within the nervous system (10, 11). These proteins are assumed to mediate intracellular responses to collapsin through a signal transduction cascade involving G protein (12) and have significant homology with the product of *unc-33* in *Caenorhabditis elegans*, mutation of which results in abnormal outgrowth of axons, leading to severe incoordination (13–15).

CRMP-2 exhibits the most ubiquitous neuronal expression among CRMPs: It appears in a majority of neurons early during development and in a selected group of adult neurons, such as pyramidal cells of the hippocampus, Purkinje cells of the cerebellum, and sensory neurons of the dorsal root

* Correspondence should be addressed to this author at the Department of Neuropathology, Faculty of Medicine, University of Tokyo, 7-3-1 Hongo, Bunkyo-ku, Tokyo 113-0033, Japan. TEL: 81-3-5841-3541, FAX: 81-3-5800-6852, E-mail: yihara@m.u-tokyo.ac.jp.

[‡] University of Tokyo.

[§] Japan Science and Technology Corp.

^{||} Nagoya City University Medical School.

¹ Abbreviations: AD, Alzheimer's disease; BAP, bacterial alkaline phosphatase; CNBr, cyanogen bromide; CRMP-2, collapsin response mediator protein-2; DRG, dorsal root ganglion; DRP, dihydropyrimidinase-related protein; DTT, dithiothreitol; ERK, extracellular signal-regulated protein kinase; GST, glutathione S-transferase; NFTs, neurofibrillary tangles; PCR, polymerase chain reaction; PHFs, paired helical filaments; PVDF, polyvinylidenedifluoride; Q buffer, 20 mM Tris-HCl, pH 8.0, 0.5 mM EDTA; SDS-PAGE, sodium dodecyl sulfate-polyacrylamide gel electrophoresis; SP buffer, 25 mM sodium phosphate, pH 6.0, 10 mM 2-mercaptoethanol, 10 mM tetrasodium pyrophosphate, 1 mM EGTA; TS buffer, 50 mM Tris-HCl, pH 7.4, 150 mM NaCl.

ganglion (DRG). In the neuron, CRMP-2 is located in the growth cone, the shaft of the axon, and the cell body (12, 16, 17).

We previously found that the immunoaffinity-purified 3F4 antigen consisted of two bands at 60 and 65 kDa on SDS-PAGE. Although both of them were proved to be CRMP-2 by sequencing, only the 65-kDa band was 3F4-reactive (9). This result raised the possibility that the 3F4-reactive protein is a modified form of the 60-kDa protein and that 3F4 recognizes this rather specific modification for AD. Another possibility is that the two are closely related isoforms presumably generated by alternative splicing, and that 3F4 recognizes only the larger one. In either case, an abundance of the 65-kDa protein characterizes the soluble fraction of the cortex in AD, and may explain the complicated picture of neuronal degeneration which occurs in the AD cortex (9): axonal and dendritic sprouting and/or retraction (18–21).

Here we show that (i) the NFT-associated 3F4 antigen represents a highly phosphorylated form of CRMP-2; (ii) the phosphorylated epitope is located carboxyl-terminal to a highly basic domain, which may be involved in protein–protein interaction or membrane association; (iii) at least three phosphorylation sites, Thr-509, Ser-518, and Ser-522, are required for full 3F4-binding; and (iv) a protein kinase with a molecular mass of 45–50 kDa is responsible for creating this phosphoepitope.

EXPERIMENTAL PROCEDURES

Materials. Unless otherwise indicated, all the reagents employed in this study were obtained from Nacalai Tesque (Kyoto, Japan) or Wako Pure Chemical Industries (Osaka, Japan). Trizma base, phenylmethylsulfonyl fluoride, *N*^α-p-tosyl-L-lysine chloromethyl ketone, diisopropyl fluorophosphate, bacterial alkaline phosphatase (*Escherichia coli*, type III; BAP), tetrasodium pyrophosphate, and dithiothreitol (DTT) were obtained from Sigma; culture medium and supplements were from Life Technologies, Inc.; antipain, pepstatin, and leupeptin were from Peptide Institute (Osaka, Japan); [γ -³²P]ATP (>3000 Ci/mmol) was from NEN Life Science Products; rabbit polyclonal anti-MAP 1/2 IgG was from Upstate Biotechnology, Inc.

cDNA Cloning of Human CRMP-2 and Construction of the Expression Vector. A pTARGET-hCRMP-2 construct containing the complete coding sequence for hCRMP-2 cDNA and a translation initiation consensus sequence (22) was created by inserting a PCR fragment amplified from a human brain Lambda ZAP cDNA library (Stratagene), using the primers 5'-tcccaggagagatgtctt-3' and 5'-ggcagagccaggactcta-3', into the pTARGET mammalian expression vector (Promega). The sequence was verified on both strands using the dideoxynucleotide chain-termination method with a SequiTherm Long-Read cycle sequencing kit (Epicentre Technologies, Madison, WI) and an Automated Laser Fluorescent DNA Sequencer (model 4000; LI-COR, Lincoln, NE).

Plasmids expressing human dihydropyrimidinase-related protein-1 (DRP-1, CRMP-1), DRP-2 (CRMP-2), DRP-3 (CRMP-4), and DRP-4 (CRMP-3) were prepared by subcloning the respective complete coding sequences (GenBank Accession Numbers D78012, D78013, D78014, and AB006713) in a pCR3 vector (Invitrogen) (23).

For all of the glutathione *S*-transferase (GST)-fusion proteins prepared in this study, the cDNA clone pTARGET-hCRMP2 was used as the template. The fusion proteins GST-Nd (amino-terminal specific domain; residues 142–194), GST-Cd (carboxyl-terminal specific domain; residues 486–528), and GST-hCRMP2 (full-length hCRMP-2) were prepared for generating monoclonal antibodies to CRMP-2. Oligonucleotide primers containing restriction endonuclease sites were designed. The PCR-amplified fragments for GST-Nd (sense primer, 5'-gtgggatccAGCGAGTGGCATAAGGGCAT-3'; antisense primer, 5'-gagaattccTATGGCGCAAT-ATCCCGGA-3') and GST-Cd (sense primer, 5'-aagggatcc-AGCAGGCTGGCTGAGCTGAGA-3'; antisense primer, 5'-gagaattcgGGCCTGCTGCTTGGCAGGAGA-3') were cleaved with *Bam*HI and *Eco*RI, and cloned into the pGEX-2TK (Amersham Pharmacia Biotech) *E. coli* expression vectors. The PCR-amplified full-length hCRMP-2 sequence (sense primer, 5'-CGCGTGAATTCCAGGAGAGAGATGT-3'; antisense primer, 5'-GGTGACACGATAGAATACTCA-3') was inserted into *Eco*RI sites of pGEX-2TK, and the orientation was verified by restriction enzyme digestion and Western blot analysis of the expressed fusion protein with the peptide antibodies to hCRMP-2.

The following GST-fusion proteins were prepared for in vitro phosphorylation: GST-Cp (residues 486–528) was prepared by inserting the same PCR-amplified fragment as that for GST-Cd into pGEX-4T-3 (Amersham Pharmacia Biotech). GST-S507A, GST-T509A, GST-T512A, GST-T514A, GST-S517A, GST-S518A, GST-T521A, and GST-S522A are all mutated forms of GST-Cp where each of the indicated Ser or Thr residues was replaced by Ala. Mutagenesis of individual codons was performed by PCR using mutated primers. The mutation in each of the inserts was verified by DNA sequencing.

Antibodies. The fusion proteins GST-Nd and GST-hCRMP2 were obtained as inclusion bodies using the standard method (24). GST-Cd was purified as a soluble protein by affinity chromatography on glutathione–Sephacryl 4B (Pharmacia Biotech) according to the manufacturer's instructions. The inclusion bodies of GST-hCRMP2 were solubilized with 8 M urea by sonication, dialyzed against 1% Triton X-100 in phosphate-buffered saline (PBS), and purified on glutathione–Sephacryl 4B. Recombinant hCRMP-2 was isolated by gel filtration on a Sephacryl S-200 HR (Pharmacia Biotech) column after proteolytic cleavage of GST-hCRMP2 with thrombin.

New monoclonal antibodies were raised against GST-Nd or GST-Cd, essentially as described (9), except that the mice were boosted twice (on days 4 and 7) and fusion was done on day 10. Recombinant hCRMP-2 was used for screening the antibody-producing hybridomas by ELISA.

Polyclonal antibody A667 was raised against a synthetic peptide of residues 147–161 of hCRMP-2 in the same way as A660 and A666 were (9).

Partial Purification of Rat CRMP-2 (rCRMP-2). rCRMP-2 was partially purified from rat brain using Western blotting with N3E (or C4G) to monitor each purification step. All steps were performed on ice or at 4 °C.

Fresh adult rat brains (20 g) were homogenized in 4 volumes of SP buffer (25 mM sodium phosphate, pH 6.0, 10 mM 2-mercaptoethanol, 10 mM tetrasodium pyrophosphate, 1 mM EGTA) containing a cocktail of protease

inhibitors (0.5 mM phenylmethylsulfonyl fluoride, 1 μ g/mL *N* $^{\alpha}$ -*p*-tosyl-L-lysine chloromethyl ketone, 1 μ g/mL leupeptin, 1 μ g/mL pepstatin, and 1 μ g/mL antipain). The homogenate was centrifuged at 300000g for 30 min at 4 °C, and the resultant supernatant was loaded onto an SP-Sepharose column (80 mL; Pharmacia) equilibrated with SP buffer. After washing the column with SP buffer, bound proteins were eluted with a linear gradient (0–250 mM) of NaCl in SP buffer. CRMP-2-containing fractions were pooled and concentrated with Centrprep (Amicon). After being exchanged into Q buffer (20 mM Tris-HCl, pH 8.0, 0.5 mM EDTA) containing 10 mM tetrasodium pyrophosphate and a cocktail of protease inhibitors using a PD-10 column (Pharmacia Biotech), the sample was applied to a Mono Q PC 1.6/5 (Pharmacia Biotech) FPLC column. Proteins were eluted with a linear gradient (0–400 mM) of NaCl in buffer Q. Fractions containing rCRMP-2 were pooled, concentrated by Centricon (Amicon), and further purified on Superdex 200 HR 10/30 (Pharmacia Biotech) using 50 mM sodium phosphate buffer (pH 7.0) as the elution buffer.

In Vitro Phosphorylation of GST-Fused hCRMP-2 Fragments. Newborn rat brains were homogenized in 4 volumes of TS buffer (50 mM Tris-HCl, pH 7.4, 150 mM NaCl) containing 200 nM okadaic acid, 10 mM 2-mercaptoethanol, 1 mM EGTA, and a cocktail of protease inhibitors (see above), and the homogenate was centrifuged at 300000g for 30 min at 4 °C. The supernatant was used as a source of protein kinase for the in vitro phosphorylation.

GST-Cp and its mutants were prepared as described for GST-Cd. In vitro phosphorylation was carried out by adding 0.15 volume of the supernatant into a reaction mixture containing GST-fusion proteins at a final concentration of 150 μ g/mL, 50 mM Tris-HCl (pH 7.5), 2 mM ATP, 5 mM MgCl₂, 0.2 mM CaCl₂, 1 μ M okadaic acid, 0.1 mM orthovanadate, 0.5 mM DTT, and a cocktail of protease inhibitors (see above). After incubation for 12 or 24 h at 37 °C, the reaction was stopped by adding the same volume of 2 \times Laemmli buffer, and the samples were boiled for 5 min. Proteins in the sample were separated on 8% Tris/tricine gel and subjected to Western blotting with 3F4.

To detect the protein kinase activity by autoradiography, the final concentration of 20 μ M [γ -³²P]ATP with a specific activity of 10 Ci/mmol was employed, and the reaction mixture was incubated for 20 min at 30 °C. The gel was dried and exposed to an imaging plate (Fuji Film, Tokyo, Japan), which was analyzed with a laser image analyzer (Fujix BAS 2000).

Immunocytochemical Studies. Immunocytochemical staining of isolated NFTs prepared from AD brains was performed using the Vectastain ABC kit (Vector Laboratories, Burlingame, CA), as described previously (25). Dephosphorylation of NFTs on a glass slide was carried out by incubating them with 10 units/mL bacterial alkaline phosphatase (BAP) in 50 mM Tris-HCl (pH 8.0) and 1 mM MgCl₂ at 65 °C for 2 h in the presence or absence of 100 mM sodium phosphate.

Immunoaffinity Purification and Immunoprecipitation. Rat brain cytosolic extract was prepared by homogenizing fresh newborn rat brains in 4 volumes of 50 mM phosphate buffer (pH 7.4) containing 10 mM tetrasodium pyrophosphate, 10 mM 2-mercaptoethanol, 1 mM EDTA, and a cocktail of protease inhibitors, followed by centrifugation at 300000g for 30 min at 4 °C. Immunoaffinity purification of the 3F4

antigen from the rat brain cytosolic extract was carried out as previously described for the TS-soluble fraction of human brain (9).

All immunoprecipitation steps were performed at 4 °C. After preclearing it with protein G-Sepharose CL-4B (Amersham Pharmacia Biotech) for 1 h, the rat brain cytosolic extract was incubated with antibody N3E or C4G for 1 h. The immunoprecipitates were recovered by incubating overnight with protein G-Sepharose CL-4B. The beads were washed 3 times with RIPA buffer (150 mM NaCl, 0.5% deoxycholic acid, 1.0% Nonidet P-40, and 50 mM Tris-HCl, pH 8.0), boiled for 5 min in Laemmli's sample buffer, and subjected to Western blotting.

Other Methods. Two-dimensional electrophoresis was performed using a nonlinear immobilized pH gradient (pH range 3.5–10) in the first dimension with Immobiline strips according to the manufacturer's instructions (Pharmacia, Uppsala, Sweden). Ten percent SDS-PAGE was used for the second dimension, and the separated proteins were transferred onto a polyvinylidenedifluoride (PVDF) membrane (Immobilon). Subsequent immunodetection was performed as described previously (26).

Transient transfection of each hCRMP clone in COS-7 cells was performed with Lipofectamine (GIBCO BRL) according to the manufacturer's instructions. Plasmids for transfection were prepared by endotoxin-free maxi-prep kits (Qiagen).

RESULTS

Further Confirmation of the 3F4 Antigen as CRMP-2. The presence of two hCRMP-2 species for the immunoaffinity-purified 3F4 antigen raised the following questions: (i) Which band represents the 572 residue hCRMP-2? (ii) What is the identity of the other band? (iii) What is the epitope of 3F4?

To address these questions, we first transiently expressed hCRMP-2 in COS-7 cells. Western blotting with A666 and A667, both of which are distinct peptide antibodies to CRMP-2 (9), showed that the transiently expressed hCRMP-2 in COS-7 cells had an apparent molecular mass of 62 kDa. 3F4, however, labeled exclusively a 66-kDa band in the cytosolic fraction of both newborn and adult rat brains (see Figure 1D). It is possible that the 66-kDa band represents a distinct isoform of CRMP-2 generated as a result of alternative mRNA splicing, or is posttranslationally modified CRMP-2. Alternatively, the 66-kDa band could be another member of the CRMP family, because at least four members of the CRMP family are known to exist in the brain, and the peptide antibodies used here could cross-react with them (see below).

To further confirm that the 3F4 antigen is indeed CRMP-2, two specific monoclonal antibodies were raised against GST/CRMP-2 fusion proteins. N3E was raised against residues 142–194, and C4G against residues 486–528. To assess the specificity of these monoclonal antibodies, each Triton X-100 (0.5%) extract of the COS-7 cells transiently transfected with hCRMP-1, -2, -3, or -4 was subjected to Western blotting. To confirm the expression of the hCRMP members, we used the peptide antibody A660, which was raised against residues 29–48 of hCRMP-2, a homologous region among the four members, and was therefore expected

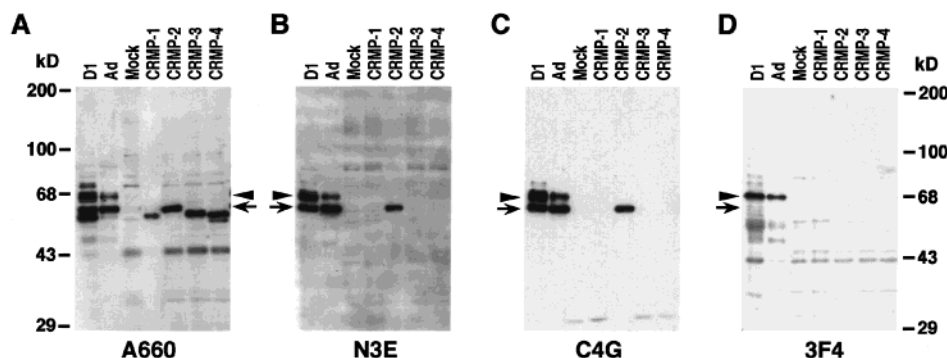


FIGURE 1: Western blot analysis of CRMPs in rat brain and transiently transfected COS-7 cells. Human CRMP-1, -2, -3, or -4 was transiently expressed in COS-7 cells. The cultured cells were washed in PBS and lysed with Tris-buffered saline (TS) containing 0.5% Triton X-100. Newborn (D1) and adult (Ad) rat brains were homogenized in TS. After high-speed centrifugation, the supernatants were subjected to Western blotting with the antibodies A660 (A), N3E (B), C4G (C), or 3F4 (D), as described under Experimental Procedures. For transfected or mock-transfected COS-7 cells, an aliquot of lysate containing 5 μ g of protein was loaded onto each lane, except for CRMP-1 sample for A660-blotting and CRMP-2 sample for N3E- or C4G-blotting, where one-tenth of this amount (equivalent to 0.5 μ g of protein) was loaded. For the rat brain samples, TS-soluble fractions from 80 μ g (for A660- or 3F4-blotting) or 20 μ g (for N3E- or C4G-blotting) wet weight of the brains were loaded onto each lane. The arrow and arrowhead in each panel indicate the 62- and 66-kDa CRMP-2, respectively. It should be noted that N3E and C4G labeled only CRMP-2, while A660 cross-reacted with other CRMPs. The apparent molecular masses are indicated on the left.

to cross-react with other members of the CRMP family (Figure 1A). The apparent molecular masses of human CRMP-1, -3, and -4 were a little smaller than that of hCRMP-2 (Figure 1A). This is also the case for mouse Ulips (11). For some unknown reason, A660 labeled hCRMP-1 much more strongly than it did other hCRMPs. As reported before (10), the bands corresponding to CRMP-1, -3, and -4 were found in the newborn rat brain, but not in the adult rat brain.

In contrast to A660, N3E and C4G showed strict specificity toward hCRMP-2: Both sensitively and specifically detected only hCRMP-2, but none of the other hCRMPs on the Western blot (Figure 1B,C). In the cytosolic fractions of both newborn and adult rat brains, N3E and C4G labeled a major band at 62 kDa, and an additional band at 66 kDa, and rather faint bands at 64 and 70 kDa, especially in the newborn rat brain extract (Figure 1B,C).

In sharp contrast, 3F4 exclusively labeled the 66-kDa band of CRMP-2 in the brain extract, but not CRMP-1, -2, -3, or -4 in transfected COS-7 cells, even if larger amounts of the sample were loaded. Thus, the 3F4 antigen is neither CRMP-1, -3, or -4 nor the major form of CRMP-2.

When rat CRMP-2 was immunoprecipitated with N3E or C4G and probed with 3F4, only the 66-kDa band was labeled (Figure 2A). In contrast, when the immunoaffinity-purified 3F4 antigen was probed with N3E or C4G, a strong band at 66 kDa and a faint band at 64 kDa were observed (Figure 2B). Altogether, these results strongly suggest that the 3F4 antigen at 66 kDa is posttranslationally modified CRMP-2.

3F4 Epitope Is Phosphorylated. The 3F4 epitope was resistant to BAP treatment at 37 $^{\circ}$ C (9), suggesting initially that the 3F4 epitope was not phosphorylation-dependent. However, when smears of NFT-rich fractions on glass slides were treated with BAP at a higher temperature (65 $^{\circ}$ C), the 3F4-immunoreactivity of NFTs decreased significantly (Figure 3A). Inclusion of sodium phosphate prevented this decrease, suggesting that this effect was a result of dephosphorylation by BAP, rather than of proteolytic degradation (Figure 3A). Furthermore, we found that the 3F4-positive band at 66 kDa disappeared gradually or rapidly, respectively, when newborn or adult rat brain homogenate was incubated

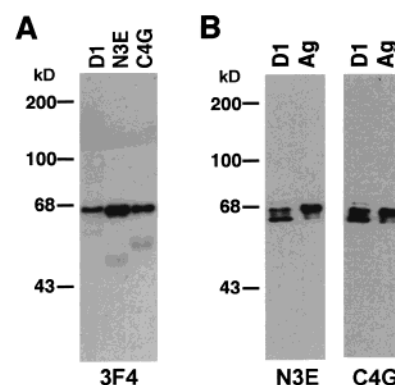


FIGURE 2: CRMP-2 as the 3F4 antigen. (A) Newborn rat brain was homogenized in 4 volumes of phosphate buffer. The high-speed supernatant was immunoprecipitated with N3E or C4G. The supernatant (left lane) and N3E- (middle lane) or C4G-immunoprecipitate (right lane) were subjected to Western blotting with 3F4. Peroxidase-conjugated rat anti-mouse kappa light chains were used as the second antibody. (B) Newborn rat brain extract (D1, left lane) and 3F4 antigen (Ag, right lane) immunoaffinity-purified from the extract were subjected to Western blotting with N3E (left) or C4G (right).

at 37 $^{\circ}$ C. Nonspecific phosphatase inhibitors such as phosphate and pyrophosphate prevented this loss of 3F4-immunoreactivity (Figure 3B). These lines of evidence strongly suggest that the 3F4 epitope is phosphorylation-dependent, although it was highly resistant to conventional treatment with BAP at 37 $^{\circ}$ C.

Longer incubation of brain extract resulted in disappearance of the 64- and 66-kDa bands, and concomitant enhancement of the 62-kDa band and emergence of a new 70-kDa band (Figure 3B). The 64- and 66-kDa bands should represent two phosphorylated isoforms of the 62-kDa CRMP-2. Possibly, the 70-kDa band may be a larger isoform of CRMP-2 arising from alternative mRNA splicing, almost indiscernible when phosphorylated but becoming discernible after dephosphorylation (see Figure 7).

Okadaic acid and microcystin-LR were able to prevent the loss of 3F4 immunoreactivity, while EGTA and vanadate were not (Figure 3C). Thus, protein phosphatase PP-1 and/or PP-2A but not phosphatase PP-2B (calcineurin) or protein

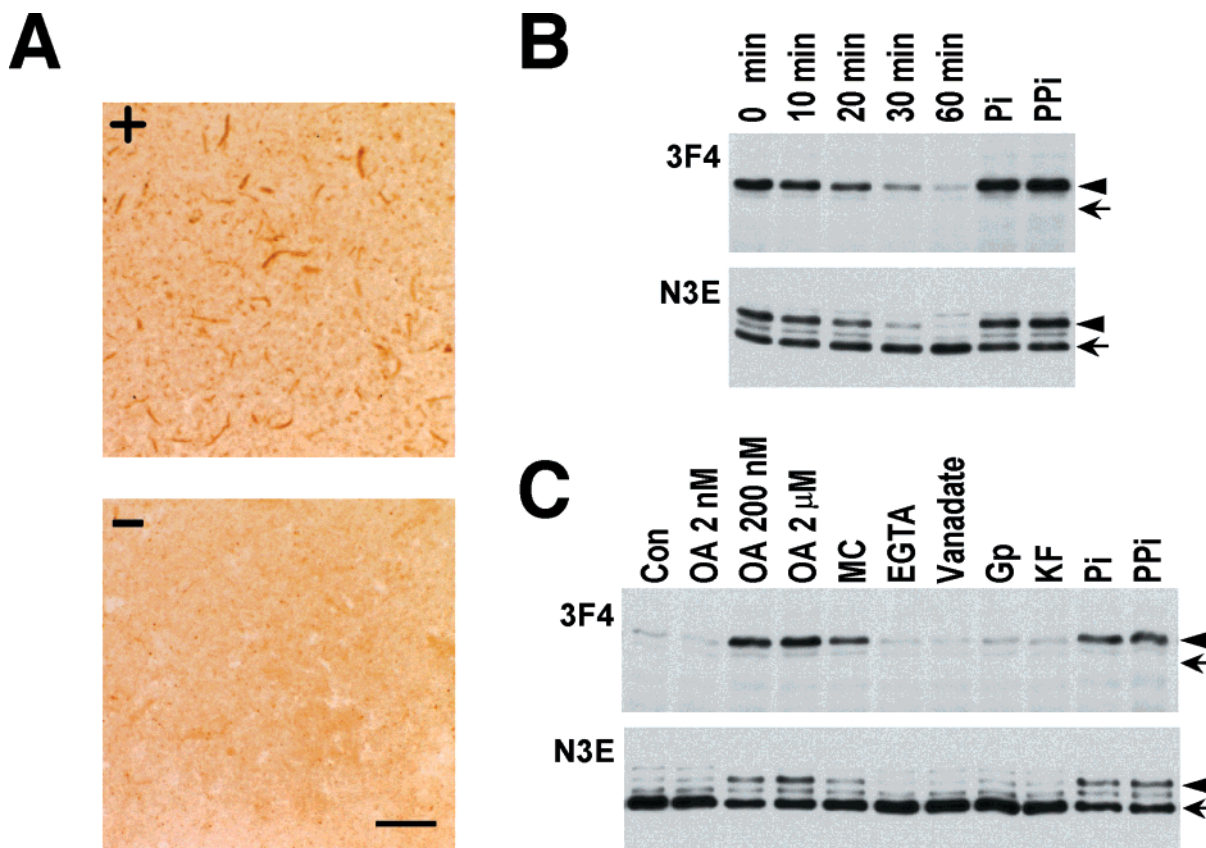


FIGURE 3: 3F4 epitope is phosphorylated. (A) An NFT preparation from an AD brain smeared onto a glass slide was incubated at 65 °C for 2 h with 10 units/mL BAP in the presence (+) or absence (−) of sodium phosphate, and stained with 3F4. Bar, 20 μ m. (B) Newborn rat brain extract was incubated in TS buffer without phosphatase inhibitors at 37 °C for the indicated periods, or for 60 min with 100 mM sodium phosphate (Pi) or 20 mM pyrophosphate (PPi). The samples were subjected to Western blotting with 3F4 (upper panel) or N3E (lower panel). (C) Newborn rat brain extract was incubated at 37 °C for 45 min in the presence of various phosphatase inhibitors: okadaic acid, 2 nM, 200 nM, or 2 μ M (OA); microcystin-LR, 200 nM (MC); EGTA, 5 mM (EGTA); vanadate, 0.5 mM (Vanadate); glycerol phosphate, 5 mM (Gp); potassium fluoride, 5 mM (KF); sodium phosphate, 100 mM (Pi); or pyrophosphate, 20 mM (PPi). Samples were subjected to Western blotting with 3F4 (upper panel) or N3E (lower panel). The arrowhead and arrow in (B) and (C) indicate phosphorylated CRMP-2 at 66 kDa and nonphosphorylated CRMP-2 at 62 kDa, respectively.

tyrosine phosphatase is likely to be responsible for dephosphorylation of CRMP-2 in vitro, and also possibly in vivo.

Mapping of the 3F4 Epitope to the Carboxyl-Terminal Portion of CRMP-2. Since this particular phosphorylation mentioned above caused a large mobility shift of CRMP-2 on SDS-PAGE, we expected that the CNBr-cleaved fragment(s) bearing this particular phosphorylation site(s) would still retain this characteristic.

We thus separated 3F4-positive and -negative rCRMP-2 by SDS-PAGE following several steps of chromatography (Figure 4A). After being transferred onto a PVDF membrane, the two bands were separately cut out and cleaved with CNBr. A panel of polyclonal (peptide) and monoclonal antibodies to CRMP-2 were used to compare the two sets of cleaved fragments on the Western blot. C4G detected a major band at 17 kDa and a minor band at 24 kDa in the CNBr digest of 3F4-negative CRMP-2, and a major band at 19 kDa and a minor band at 26 kDa in the digest of the 3F4-positive CRMP-2. As expected, 3F4 labeled the 19- and 26-kDa bands only in the digest of 3F4-positive CRMP-2 (Figure 4B). Probably, the previous failure to detect positive CNBr fragments using 3F4 is due to the use of the avidin-biotin method (9), instead of the enhanced chemiluminescence method. CNBr cleavage gives rise to a carboxyl-terminal 135-residue fragment which has a theoretical

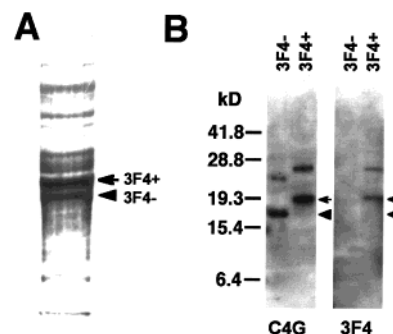


FIGURE 4: Mapping of the 3F4 epitope to the carboxyl-terminal portion of CRMP-2. (A) Partially purified rCRMP-2 was separated into 3F4-positive (3F4+; arrow) and 3F4-negative (3F4−; arrowhead) species by SDS-PAGE, transferred onto Immobilon, and stained with Coomassie brilliant blue. (B) Each 3F4-positive or -negative band was separately cut out, and cleaved with CNBr. Fragments generated were separated on a 15% Tris/tricine gel and subjected to Western blotting with C4G (left panel) or 3F4 (right panel). The arrow and arrowhead indicate the positions of 19- and 17-kDa bands, respectively. The bands at 24 and 26 kDa probably represent a 197-residue fragment (see Figure 6) resulting from incomplete CNBr cleavage.

molecular mass of 14.5 kDa and spans the C4G epitope (see Figure 5). The 17- (in 3F4-negative CRMP-2) and 19-kDa (in 3F4-positive one) bands should represent the 135-residue fragment. When cleavage is incomplete, a 197-residue

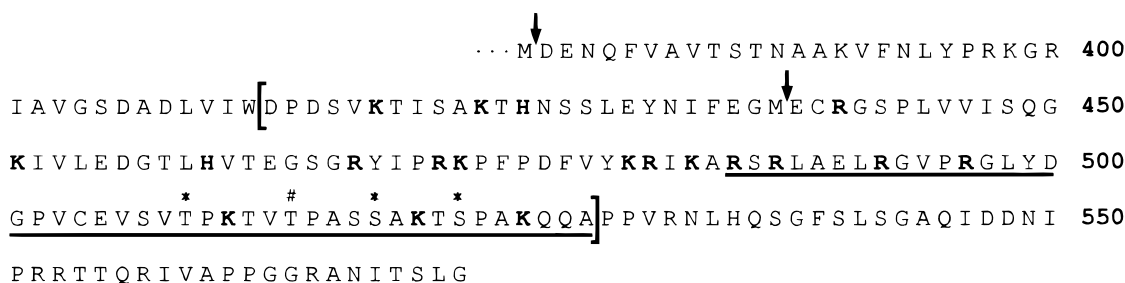


FIGURE 5: Carboxyl-terminal 198 amino acid sequence of human CRMP-2. Arrows indicate the Met residues cleaved with CNBr. Phosphorylation sites essential (*) and not essential (#) for 3F4 recognition are marked. The brackets indicate the carboxyl-terminal-specific region, within which the basic amino acids are shown in boldface letters. The portion used for generating C4G and for in vitro phosphorylation is underlined.

fragment remains. The 24- or 26-kDa bands arose most likely from such incomplete CNBr cleavage of CRMP-2 (see Figure 5). This experiment indicated that the 3F4 epitope is located in the 135-residue portion of the carboxyl terminus, and may be close to the epitope of C4G (Figure 5).

Phosphorylation of Three Sites, Thr-509, Ser-518, and Ser-522, Is Required for Full 3F4 Binding. The 135-residue fragment of the carboxyl terminus was digested with endopeptidase Asp-N or *Achromobacter lyticus* protease I. Mass spectral analysis of the digests showed that two or more sites are phosphorylated in the region of residues 505–525 (data not shown). This region happened to be located within the Cd portion (residues 486–528) used for generating C4G. This led us to use the GST-fused Cd as a substrate and rat brain extract as the protein kinase source for creating the 3F4 phosphoepitope. Rat brain extract did create the 3F4 phosphoepitope on this fragment as well as on endogenous CRMP-2. Except for Ser-486, a site not phosphorylated according to mass spectral analysis, any single residue or any combination of the other eight Ser and Thr residues is a candidate for this distinct phosphorylation specifically recognized by 3F4.

To identify the phosphorylated residue(s) required for 3F4 binding, we adopted a site-directed mutagenesis strategy to alter the codes for these Ser and Thr residues. These Ser or Thr residues were substituted by Ala, and the mutant fragments were designated as S507A, T509A, T512A, T514A, S517A, S518A, T521A, or S522A (Figure 6A). The GST-fused wild-type and mutant fragments were purified from *E. coli* and subjected to in vitro phosphorylation. Newborn rat brain extract created the 3F4 phosphoepitope on all the mutant fragments in addition to the wild-type one (Figure 6B). However, semiquantitative assessment indicated that the extent of 3F4-immunoreactivity of T509A, S518A, or S522A was only one-fourth to one-sixth as compared with that of the others (Figure 6B). Because the concentrations of these fusion proteins were the same, the decreased 3F4 binding of these mutants was attributable to the absence of phosphorylation at the corresponding residues. Thus, phosphorylation of all three sites, Thr-509, Ser-518, and Ser-522, is required for the creation of the 3F4 epitope; the first and the last are proline-directed sites (see Figure 6A).

We cannot, however, exclude the following two possibilities: mutation of certain Ser or Thr residues may affect the phosphorylation of other sites in the 3F4 epitope; or mutation itself may cause a decrease in 3F4 binding. In this context, it must be pointed out that in addition to the three 3F4 epitope-related residues, other Ser or Thr residues examined

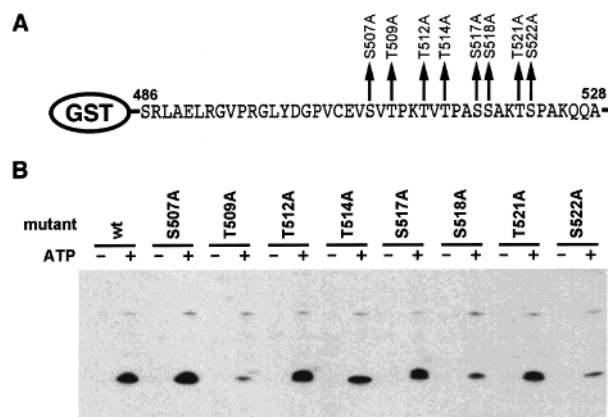


FIGURE 6: In vitro phosphorylation of the carboxyl-terminal portion of hCRMP-2 and its mutants. (A) Schematic representation of GST-fused residues 486–528 of hCRMP-2 and site-directed mutants. Ser or Thr was replaced with Ala in each of the mutants at the indicated sites. (B) In vitro phosphorylation of wild-type (wt) and mutated proteins in the absence (–) or presence (+) of 2 mM ATP using newborn rat brain extract as a protein kinase source. Samples were subjected to Western blotting with 3F4. A faint band at 66 kDa probably represents the endogenous CRMP-2 included in the enzyme source.

here could also be phosphorylated in vitro or in vivo. Thr-514, for example, is most likely to be phosphorylated in vitro (and may also be so in vivo). The T514A mutation did not affect the formation of the 3F4 epitope in vitro, but prevented a mobility shift on SDS–PAGE after in vitro phosphorylation (Figure 6B). Thus, without phosphorylation on Thr-514, the mobility shift of CRMP-2 would not occur to the full extent.

Western blot analysis following two-dimensional polyacrylamide gel electrophoresis (2D-PAGE) of newborn rat brain cytosol supported the above view: phosphorylation of all three aforementioned sites is required for full 3F4 binding. Rat CRMP-2 isoforms fell into two groups by 2D-PAGE-based Western blotting with C4G (or N3E; data not shown), with the low-molecular-mass (62–66 kDa) group being predominant. Eight isoforms were identifiable in the low-molecular-mass group (designated species 1–8 in Figure 7). These isoforms can be postulated to represent nonphosphorylated and phosphorylated CRMP-2 with a difference of one phosphate between neighboring species (17). Species 1, 2, and 3 are presumed to be nonphosphorylated, mono-phosphorylated, and diphosphorylated forms, respectively. These gave stronger signals than species 4–8 on Western blots with C4G or N3E (data not shown), while they exhibited no (species 1) or much weaker (species 2 and 3)

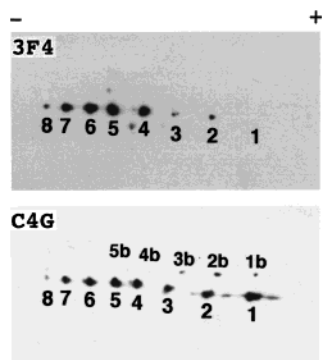


FIGURE 7: Two-dimensional PAGE of newborn rat brain extract and subsequent Western blotting with 3F4 or C4G. Cytosolic fraction from 10 mg (for 3F4) or 2 mg (for C4G) wet weight of newborn rat brain tissue was subjected to two-dimensional PAGE, followed by Western blotting with 3F4 or C4G. Two groups, with low (1–8) and high (1b–5b) molecular masses of CRMP-2, are recognized. Phosphorylated forms are numbered 2–8, with species 8 being the most phosphorylated one. The spot above species 5 on the 3F4 blot may represent a phosphorylated high-molecular-mass CRMP-2, because a corresponding spot became discernible by ECL detection on the C4G blot after longer exposure.

signals on Western blots with 3F4 (Figure 7). Careful comparison of 2D-PAGE and SDS-PAGE showed that species 1 and 2 corresponded to the 62-kDa band, species 3 to the 64-kDa band, and species 4–8 to the 66-kDa band. The isoforms in the high-molecular-mass group (designated species 1b–5b in Figure 7) are likely to be differentially phosphorylated 70-kDa CRMP-2. They are expressed only at lower levels, but some isoforms with multiple phosphorylation sites were observed on 3F4-blotting by longer exposure.

Characterization of Protein Kinase(s) Responsible for the Phosphorylation of CRMP-2. On gel filtration chromatography of rat brain extract, a major protein kinase activity with an apparent molecular mass of about 45–50 kDa was eluted (Figure 8A). The 3F4 phosphopeptide was created by this active fraction (Figure 8C). In particular, the protein kinase was not cofractionated with MAP kinases ERK1/ERK2 by Mono-S column chromatography (Figure 8B). Glycogen synthase kinase (GSK)-3 β is also not responsible for the protein kinase activity (data not shown). The protein kinase activity is also present in COS-7 cells, suggesting that it is not central-nervous-system-specific, although 3F4 immunoreactivity was indiscernible in the transiently transfected COS-7 cells (Figure 1D). The CRMP-2 kinase(s) was (were) activated by heparin (Figure 8D), and sensitive to salt concentration, as the presence of 200 mM NaCl significantly inhibited its activity (data not shown).

DISCUSSION

The present study clearly shows that the monoclonal antibody 3F4, which strongly stains NFTs in AD brains, recognizes a highly phosphorylated form of CRMP-2. Phosphorylation of the sites identified here may play important roles in the regulation of CRMP-2 functions *in vivo*, and thus in neurite extension. Semiquantitation by densitometry of the phosphorylated and nonphosphorylated forms indicated that the former amounts to approximately half of the total CRMP-2 in the newborn and one-third of that in the adult rat brain (see also Figures 1–3). The

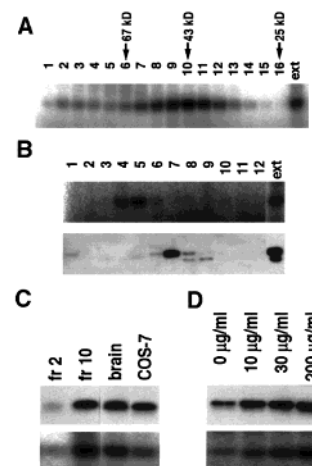


FIGURE 8: Characterization of kinase(s) responsible for the phosphorylation of CRMP-2. (A) A 45–50-kDa protein kinase phosphorylated CRMP-2. Gel filtration fractions of newborn rat brain cytosolic extract from a Superdex-75 FPLC column were analyzed for kinase activities using GST-fused residues 486–528 of hCRMP-2 as the substrate. Each reaction mixture was subjected to SDS-PAGE and autoradiography. Relative molecular masses are indicated above the fraction numbers. ext, newborn rat brain extract. (B) MAP kinases are not responsible for the phosphorylation of CRMP-2. Newborn rat brain extract was separated on a Mono-S FPLC column. The fractions were subjected to a kinase assay (upper panel, autoradiography) and Western blotting using anti-ERK1/ERK2 antibody (lower panel). (C) The kinase activities in gel filtration fractions 2 (fr 2) and 10 (fr 10) in (A) and in the cytosolic extracts from newborn rat brain (brain) and COS-7 cells (COS-7). (D) The CRMP-2 kinase(s) is (are) activated by 10–200 μ g/mL heparin. Kinase activities in newborn rat brain extract were examined in the absence or presence of 10, 30, and 200 μ g/mL heparin. Kinase activities in (C) and (D) were analyzed by *in vitro* phosphorylation of the GST-fused residues 486–528 of hCRMP-2, followed by Western blotting with 3F4 (upper panel) or by autoradiography (lower panel).

carboxyl-terminal portion (residues 507–522) appears to be the primary region phosphorylated *in vivo*, because preliminary 2D-PAGE analysis showed that 5–7 sites in this small portion could be phosphorylated by the *in vitro* phosphorylation protocol, accounting for almost all of the phosphorylation sites of CRMP-2 *in vivo* (Gu, Y., and Ihara, Y., unpublished data; see Figure 7). Many phosphorylation sites clustered within this small region prompted us to carefully examine the characteristics of this and neighboring domains. Residues 412–527 exhibited relatively low homology among the members of the CRMP family, and this region is thus called the “C-terminal-specific region” (11). In all four members of the CRMP family, this region is rich in basic residues. Nineteen of the 115 residues are basic, resulting in a calculated *pI* of about 12.5 for this domain of CRMP-2 (see Figure 5). Similarly, 20, 18, or 20 basic residues are present in this specific domain of CRMP-1, -3, or -4, respectively. Moreover, for all the members of the CRMP family, a cluster of 10 basic residues exists in a 30 amino acid stretch (residues 467–496 of CRMP-2) just amino-terminal to the phosphorylated region of CRMP-2 (see Figure 5). The “C-terminal-specific region” seems critical neither to the interaction among members of the CRMP family (27) nor for direct mediation of the collapsin signal (12). It is tempting to speculate that this region is a regulatory domain of the CRMP molecules. Phosphorylation at several sites in this region may allow an interaction with the neighboring

basic domain, thereby inhibiting the interaction of CRMPs with other proteins or membrane, or changing the three-dimensional conformation of the CRMP tetramer.

The phosphorylation sites recognized by 3F4 are resistant to BAP, while some other sites are not: Treatment of purified 3F4 antigen with BAP at 37 °C caused a mobility shift on SDS-PAGE but little loss of 3F4 immunoreactivity (9). Decreased immunoreactivity was first observed on the BAP-treated NFT preparation, presumably because (i) the phosphorylated CRMP-2 becomes partially unfolded at 65 °C and BAP can gain access to the phosphorylation sites, and (ii) immunocytochemistry may be even more sensitive to the loss of epitope than Western blotting. In contrast to its resistance to BAP treatment, CRMP-2 appeared to be a good substrate for endogenous protein phosphatases in the brain: the 3F4-positive band at 66 kDa was found to rapidly disappear when the adult rat brain homogenate was incubated at 37 °C. This may explain why the 3F4 epitope was undetectable in adult rat brain in the previous study, in which we included no phosphatase inhibitors during sample preparation (9). Rapid dephosphorylation of CRMP-2 by endogenous phosphatases could occur in human brains during the postmortem period. Nevertheless, the levels of the 3F4 antigen, a phosphorylated form of CRMP-2, were significantly increased in the cytosolic fraction of AD brain homogenates compared with that in the case of control brains (9). This may be consistent with the previous observation that the activities of protein phosphatases, especially PP1 and PP2A, are significantly suppressed in the AD brain (28).

To elucidate the role of increased levels of phosphorylated CRMP-2 in AD brain, it is essential to learn where it is localized in the central nervous system, and when it appears during neuronal development or differentiation. However, we have been unable to unambiguously visualize the localization of phosphorylated CRMP-2 in control human brains or fetal and adult rat brains by immunocytochemistry. This may be due to the presence of too small amounts of cytosolic phosphorylated CRMP-2 and/or to its unusual vulnerability to fixation, and to the relatively low affinity of 3F4. We have also examined the expression of 3F4 epitope in cultured cells. Retinoic acid-induced differentiation of SH-SY5Y cells led to a large increase of the 62-kDa species but no increase in the 3F4-reactive phosphorylated species, as judged by Western blotting (data not shown). A suggestion about the possible roles of phosphorylated CRMP-2 comes from its proportion in the rat brain during development: In the fetal rat brain, it exists obviously at higher levels, as compared with those in the adult rat brain (see Figure 1). This may suggest that the phosphorylated form is abundant in the developmental stage involved in actively extending neurites. Thus, the significantly higher levels of the phosphorylated CRMP-2 in AD brains may reflect an attempt of the remaining neurons to compensate for the neuronal loss. In this context, it is of note that NFT-bearing neurons show more extensive dendritic trees than NFT-free neurons in CA1 of the hippocampus in AD (29).

The increased levels of cytosolic phosphorylated CRMP-2 point to the possibility that the biochemical equilibrium shifts to phosphorylation in the neurons of AD brain. This balance between phosphorylation and dephosphorylation in a given cell should explain why the COS-7 lysate catalyzes the formation of the 3F4 epitope *in vitro*, whereas transiently

transfected COS-7 cells cannot phosphorylate CRMP-2 to a significant level.

Tau shares with CRMP-2 the characteristic of high level of phosphorylation in NFTs. Increased kinase activities have been suggested as one possible cause of this pathologic lesion. Several kinases are involved in tau phosphorylation, among which mitogen-activated protein kinase (MAP kinase), GSK-3 β , cdc2/cyclin B1, and cyclin-dependent kinase (CDK) 5 are proline-directed kinases (30). It is intriguing to investigate if any of these kinases are also responsible for CRMP-2 phosphorylation. MAP kinases and GSK-3 β were investigated in this study because their apparent molecular masses are close to that of the kinase responsible for CRMP-2 phosphorylation. Furthermore, 3F4-epitope-related phosphorylation sites are consistent with their consensus sequences. However, neither of the kinases appear to be a CRMP-2 kinase(s). Thus, the identity of "CRMP-2 kinase(s)" responsible for the phosphorylation of the 3F4 epitope remains elusive. Characterization of the protein kinase(s) may shed some light as to how extracellular signals of semaphorin/collapsin are relayed to intracellular events, and also how increased levels of phosphorylated CRMP-2 are related to the formation of numerous, abnormally growing and apparently dying-back neuronal processes observed in AD brains (9).

ACKNOWLEDGMENT

We thank Dr. T. Yamazaki for the immunofluorescence observations, Dr. H. Yoshida for his critical reading of the manuscript, and Mrs. M. Anzai for typing the manuscript.

REFERENCES

- Lee, V. M., Balin, B. J., Otvos, L., Jr., and Trojanowski, J. Q. (1991) *Science* 251, 675–678.
- Kondo, J., Honda, T., Mori, H., Hamada, Y., Miura, R., Ogawara, M., and Ihara, Y. (1988) *Neuron* 1, 827–834.
- Watanabe, A., Takio, K., and Ihara, Y. (1999) *J. Biol. Chem.* 274, 7368–7378.
- Gomez-Isla, T., Hollister, R., West, H., Mui, S., Growdon, J. H., Petersen, R. C., Parisi, J. E., and Hyman, B. T. (1997) *Ann. Neurol.* 41, 17–24.
- Hutton, M., Lendon, C. L., Rizzu, P., Baker, M., Froelich, S., Houlden, H., Pickering-Brown, S., Chakraverty, S., Isaacs, A., Grover, A., Hackett, J., Adamson, J., Lincoln, S., Dickson, D., Davies, P., Petersen, R. C., Stevens, M., de Graaff, E., Wauters, E., van Barden, J., Hillebrand, M., Joosse, M., Kwon, J. M., Nowotny, P., Che, L. K., Norton, J., Morris, J. C., Reed, L. A., Trojanowski, J., Basun, H., Lannfelt, L., Neystat, M., Fahn, S., Dark, F., Tannenberg, T., Dodd, P. R., Hayward, N., Kwok, J. B. J., Schofield, P. R., Andreadis, A., Snowden, J., Craufurd, D., Neary, D., Owen, F., Oostra, B. A., Hardy, J., Goate, A., van Swieten, J., Mann, D., Lynch, T., and Heutink, P. (1998) *Nature* 393, 702–705.
- Poorkaj, P., Bird, T. D., Wijsman, E., Nemens, E., Garruto, R. M., Anderson, L., Andreadis, A., Wiederholt, W. C., Raskind, M., and Schellenberg, G. D. (1998) *Ann. Neurol.* 43, 815–825.
- Spillantini, M. G., Murrell, J. R., Goedert, M., Farlow, M. R., Klug, A., and Ghetti, B. (1998) *Proc. Natl. Acad. Sci. U.S.A.* 95, 7737–7741.
- Goedert, M., Crowther, R. A., and Spillantini, M. G. (1998) *Neuron* 21, 955–958.
- Yoshida, H., Watanabe, A., and Ihara, Y. (1998) *J. Biol. Chem.* 273, 9761–9768.
- Wang, L. H., and Strittmatter, S. M. (1996) *J. Neurosci.* 16, 6197–6207.
- Byk, T., Ozon, S., and Sobel, A. (1998) *Eur. J. Biochem.* 254, 14–24.

12. Goshima, Y., Nakamura, F., Strittmatter, P., and Strittmatter, S. M. (1995) *Nature* 376, 509–514.
13. Hedgecock, E. M., Culotti, J. G., Thomson, J. N., and Perkins, L. A. (1985) *Dev. Biol.* 111, 158–170.
14. Hedgecock, E. M., Culotti, J. G., Hall, D. H., and Stern, B. D. (1987) *Development* 100, 365–382.
15. Desai, C., Garriga, G., McIntire, S. L., and Horvitz, H. R. (1988) *Nature* 336, 638–646.
16. Minturn, J. E., Fryer, H. J., Geschwind, D. H., and Hockfield, S. (1995) *J. Neurosci.* 15, 6757–6766.
17. Byk, T., Dobransky, T., Cifuentes-Diaz, C., and Sobel, A. (1996) *J. Neurosci.* 16, 688–701.
18. Probst, A., Basler, V., Bron, B., and Ulrich, J. (1983) *Brain Res.* 268, 249–254.
19. Masliah, E., Mallory, M., Hansen, L., Alford, M., DeTeresa, R., and Terry, R. D. (1993) *Am. J. Pathol.* 142, 871–882.
20. McKee, A. C., Kowall, N. W., and Kosik, K. S. (1989) *Ann. Neurol.* 26, 652–659.
21. Benzing, W. C., Ikonotovic, M. D., Brady, D. R., Mufson, E. J., and Armstrong, D. M. (1993) *J. Comp. Neurol.* 334, 176–191.
22. Kozak, M. (1987) *Nucleic Acids Res.* 15, 8125–8148.
23. Hamajima, N., Matsuda, K., Sakata, S., Tamaki, N., Sasaki, M., and Nonaka, M. (1996) *Gene* 180, 157–163.
24. Harlow, E., and Lane, D. (1988) in *Antibodies: a laboratory manual* (Harlow, E., and Lane, D., Eds.) pp 90–91, Cold Spring Harbor Laboratory, Cold Spring Harbor, NY.
25. Ihara, Y., Abraham, C., and Selkoe, D. J. (1983) *Nature* 304, 727–730.
26. Gu, Y., Oyama, F., and Ihara, Y. (1996) *J. Neurochem.* 67, 1235–1244.
27. Wang, L. H., and Strittmatter, S. M. (1997) *J. Neurochem.* 69, 2261–2269.
28. Gong, C. X., Singh, T. J., Grundke-Iqbal, I., and Iqbal, K. (1993) *J. Neurochem.* 61, 921–927.
29. Gertz, H. J., Kruger, H., Patt, S., and Cervos-Navarro, J. (1991) *Brain Res.* 548, 260–266.
30. Johnson, G., and Hartigan, J. (1998) *Alzheimer's Dis. Rev.* 3, 125–141.

BI992323H